MONITORING OF SINGLE-TRACK DEGRADATION IN THE PROCESS OF SELECTIVE LASER MELTING

I. Zhirnov[1,3], M. Doubenskaia[2], D. Kotoban[1]

[1]Moscow State University of Technology "STANKIN", Vadkovsky per. 3a, 127055 Moscow, Russia
[2]DIPI Laboratory, Université de Lyon, Ecole Nationale d'Ingénieurs de Saint-Etienne (ENISE), Saint-Etienne, France
[3] Physical Measurement Laboratory, National Institute of Standards and Technology, Gaithersburg, MD 20899

Abstract

Selective laser melting machines provide the optimal working parameters for manufacturing during the process. However, the laser interaction with metal powder is an unstable. The gasdynamic flows make powder particles move and escape from the melt pool. This phenomenon leads to an irregular distribution of the material volume being remelted. Since the energy is constant during the process, single-tracks with different geometry are appeared and their superposition forms the 3D-object. To detect the process abnormality of stable track formation there was developed a control system based on morphological analysis of thermal image obtained by IR-camera. The temperature field distribution along the image matrix's row with the maximum temperature was used as influencing factor on stable track formation. Roughness was reduced from 39.9 to 6.6 μm by using control system with the same process parameters. The obtained results can be applied in industrial SLM machines with the integrated active control system.

Introduction

To monitor melting of the powder, consolidation and solidification of the material in a 100 μm melt pool, a time resolution of about 10 μs is required, and for controlling the entire production cycle and process stability, the resolution should be at the millisecond level [1, 2]. Therefore, optical monitoring is methodologically difficult due to the wide time and spatial span and complexity of the process parameters: the temperature range (500-3500°C), the high heating and cooling rate (10^3-10^8 °C/s), small size of the heating zone (0.1 - 5 mm), the effect of radiation from a laser jet, plasma, etc., a sharp change of the optical and thermal properties, etc [3, 4].

Before direct production of a particular product, selective laser melting parameters are searched and optimized [5, 6]. As a rule, from the whole range of factors affecting the quality of the part, the most significant ones are chosen:

- laser power;
- scanning speed;
- the thickness of the powder layer and its granulometry.

Then parametric analysis is performed, determining the most optimal values for each factor. The criterion for finding the production parameters for any product is the formation of stable, dense (no voids and pores) of single tracks having the regular geometric shape and good

metallurgical connection with the substrate. The product obtained by selective laser melting is a superposition of single tracks (Figure 1) [7].

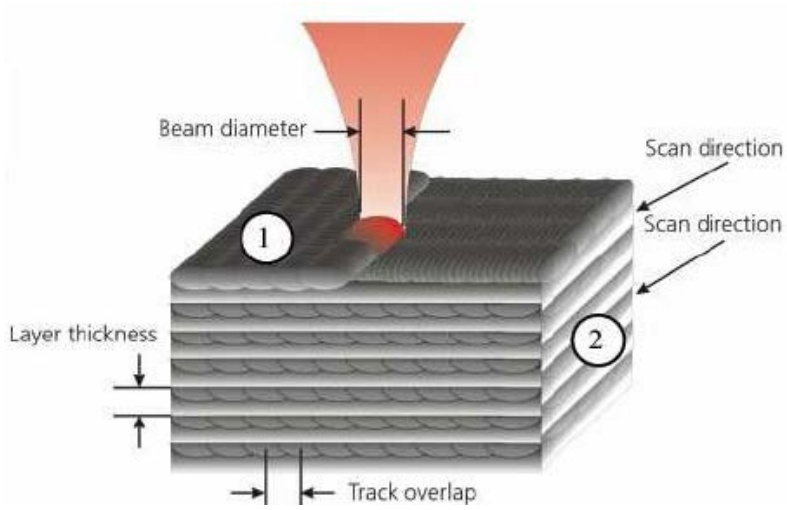

Figure 1. Plan of the product formation process [7]

The quality of the final object will consist of the quality of each track, so the mode debugging is conducted on single tracks, while saving time and material [8].

When performing the parametric analysis, it is possible to obtain the dependence of the quality of a single track on the melting parameters. For example, the formation of stable tracks depending on scanning speed and laser power (Figure 2) [5].

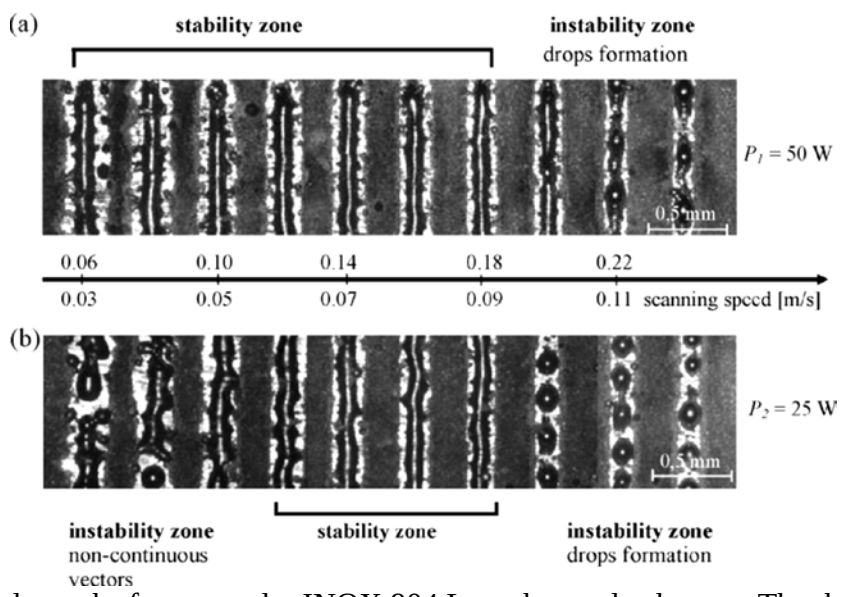

Figure 2. Single tracks from powder INOX 904 L on the steel substrate. The thickness of the powder layer is 50 μm [5]

As a rule, the search for optimal melting modes cannot fully ensure the constant quality of the formation of single tracks during the product production. A multiplicity of influencing factors

and a long production time require constant monitoring of the laser processing zone (the track forming zone).

One way to solve this problem can be the use of a high-speed infrared camera integrated into an industrial machine. The IR-camera signal is able to diagnose the effect of drops formation during SLM [9].

The reason for the drops formation at a high scanning speed is probably the insufficient amount of material involved in the melting pool (due to lack of energy). On the one hand, high scanning speeds facilitate creation of tracks of a given width and increase in productivity. On the other hand, the optimal mode parameters are determined by the quality of the fused material, the quality of the obtained layers and the 3D-objects [9].

Experimental Setup

Today, measurements of temperature fields, geometry of the melting pool shape and thermocycling in the high-speed melting processes of powder materials are performed by non-contact optical diagnostics using an IR-camera, a pyrometer and a CCD camera, individually and as part of an integrated system.

Non-contact optical diagnostics of the melting process of powder materials is conducted in two different versions:

- installation of optical measuring tools directly within the working area, at an angle of at least 45° relative to the laser exposure zone;
- placement of optical measuring tools coaxially to laser radiation within one optical path.

In this study, the first method of placements the measuring tools was used, since an IR-camera operating within the wavelength range of 3-5 μm was used as an information measuring system, and the optical system of the installation was designed for 1.07 μm (Figure 3).

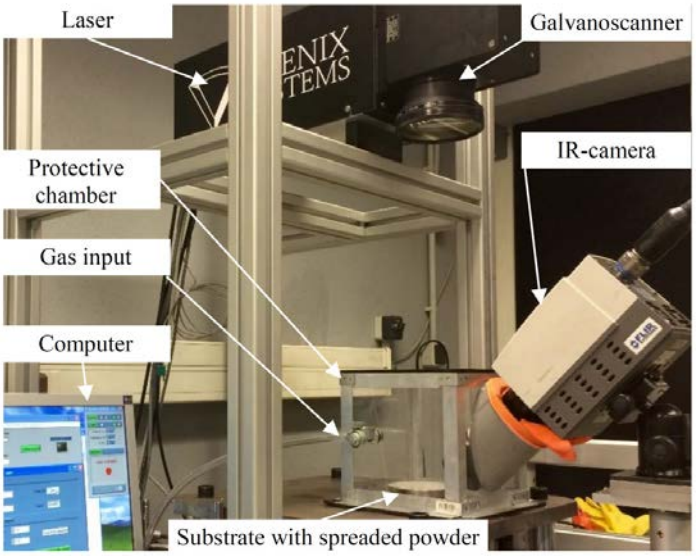

Figure 3. Plan of optical diagnostics of the melting process of powder materials.

The infrared camera FLIR Phoenix RDAC ™ (Flir, USA) was used as a measuring tool. The infrared camera used in the study has a full resolution of 320x256 pixels at a frame rate of

345. To increase the frame rate to 2278, the resolution was reduced to 128x64 pixels. The exposure time is 0.01 msec, 87 pixels of the image corresponded to one millimeter of the surface.

Results and Discussion

The true temperature within the laser processing zone is an important parameter in determining the physical properties of the material. The proposed method can be used to control the geometry and temperature fields during SLM, which in turn will help to improve the quality and accuracy of products. High-speed video recording of SLM process is an effective tool for understanding this very complex and fast process at the micro level. Figure 4 shows imaging of the motion of particles of molybdenum powder in SLM. The mechanism of the denudation zone (Figure 5) formation consists in the formation of a gas-dynamic flux in the laser exposure zone induced by the draft (stack effect) by evaporation flux from the melt pool surface. At the same time, the powder particles are involved along with the gas flux, incorporated into the melting pool or being thrown out in the form of sparks. Evaporation flux, apparently, directly depends on the temperature field on the surface of the melting pool, i.e. it is related to the process parameters. Simple conclusions show that the evaporation, coupled with the hydrodynamic behavior of the melting pool under the influence of laser radiation, form limitations in the technology of laser layer-by-layer 3D synthesis of the parts, as well as in other laser technologies. A similar result was obtained in [10], where the authors found similar effects (similar to Bernoulli effect) and described the medium gas dynamics behavior in SLM.

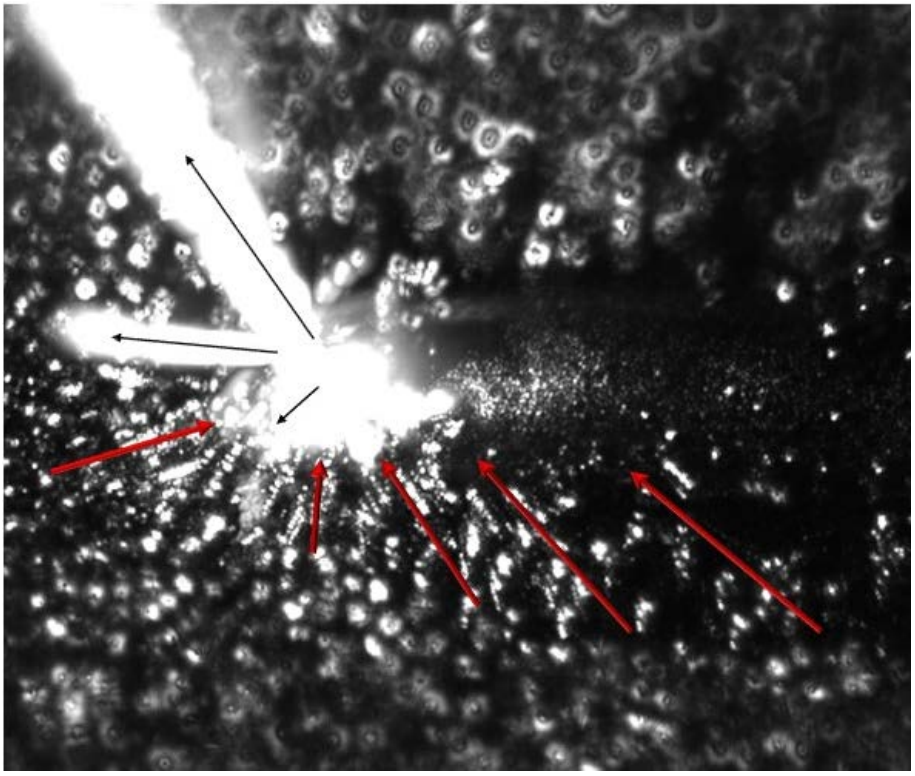

Figure 4. Overlay of 8 consecutive frames. Imaging of the motion of particles of molybdenum powder in SLM.

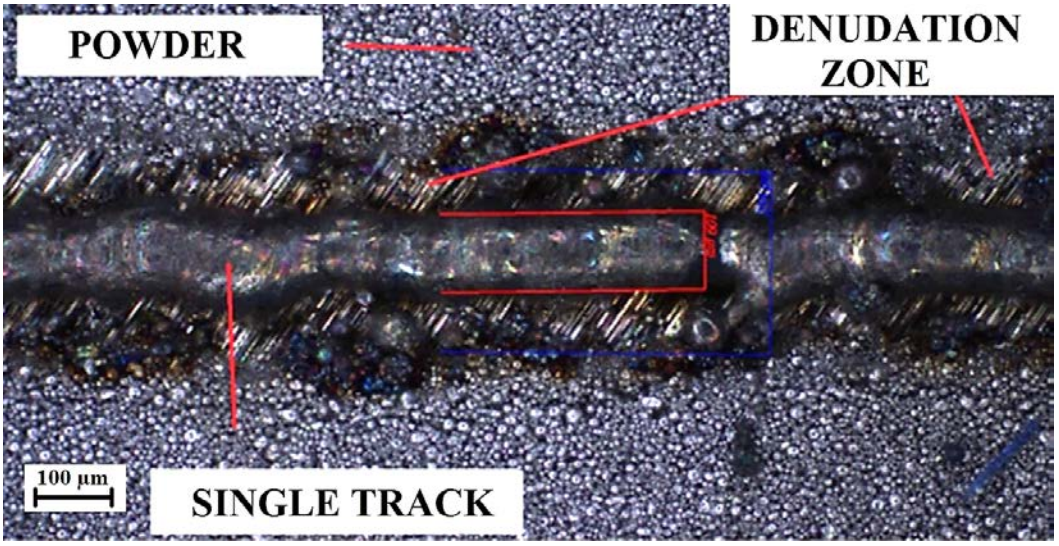

Figure 5. Image of a single track after melting.

Images obtained using the IR-camera that observes the laser radiation zone during SLM contain information about the moment of formation of a specific track. During the experiments, it was found that fragmentation of a melting isotherm leads to the formation of spheres (an unstable single track) during the metal powder melting. This is primarily due to the low energy input, as seen in the thermal image (Figure 6a), the maximum temperature for scanning speed of 300 mm/s does not exceed 2000°C, while the maximum temperature for 100 mm/s is within 2650°C. In this case, a small amount of heat is not enough to melt not only powder, but also the substrate. The lack of metallurgical connection leads to a low heat dissipation into the cast material, so the liquid melting pool on the surface of a powder layer cools more slowly and expands. Surface tension forces lead to an increase of the contact angle. A liquid track is formed on the surface, but because of the Rayleigh-Plateau instability, it fails, and spheres are formed [11-13]. As a result, an unstable track is formed (Figure 6b).

Thus, by establishing control over the melting isotherm geometry on the thermal image, namely its integrity, it is possible to control track formation stability within the laser exposure zone. Even with setting of optimal melting modes, it is impossible to ensure the constancy of high-quality product formation (track superposition) over a long manufacturing time. Uneven spreading of the powder layer, unstable distribution of laser energy, inaccuracy in the movement of the units and the mechanisms of the working machine – all this can lead to local changes in the zone of track formation.

Figure 7 shows two data sets A and B for two images. The size of each matrix is 128x64. If we construct a two-dimensional distribution of each of the matrices, then we obtain images similar to those displayed in the interface of the IR-camera program (Figure 8).

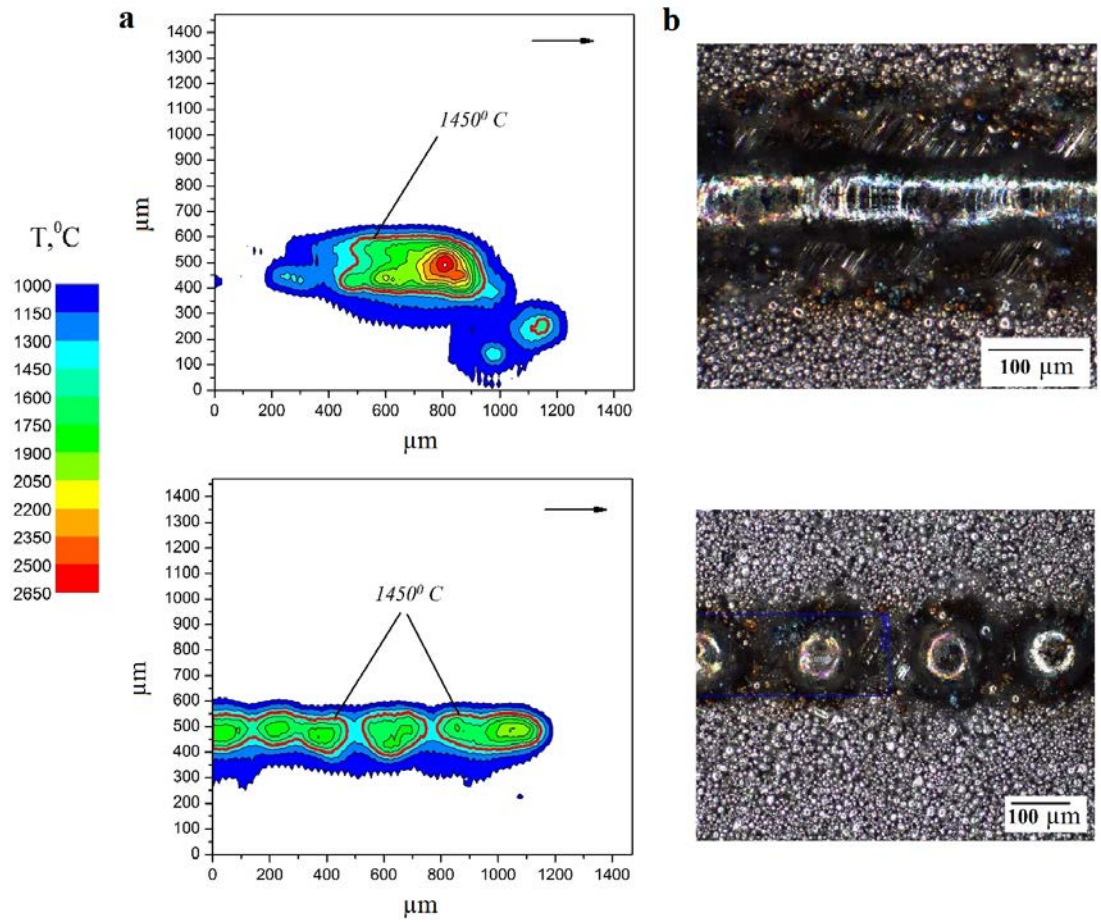

Figure 6. Isotherms obtained using the IR-camera (a); single tracks on the substrate (b). Melting parameters: laser power – 30 W, scanning speed above – 100 mm/s, below – 300 mm/s

A :=

	1	2	3	4	5
1	$1.261\cdot10^3$	985	$1.217\cdot10^3$	952	$1.201\cdot10^3$
2	$1.291\cdot10^3$	$1.004\cdot10^3$	$1.227\cdot10^3$	987	$1.209\cdot10^3$
3	$1.328\cdot10^3$	$1.045\cdot10^3$	$1.286\cdot10^3$	$1.017\cdot10^3$	$1.268\cdot10^3$
4	$1.416\cdot10^3$	$1.093\cdot10^3$	$1.293\cdot10^3$	$1.048\cdot10^3$	$1.272\cdot10^3$
5	$1.583\cdot10^3$	$1.185\cdot10^3$	$1.354\cdot10^3$	$1.084\cdot10^3$	$1.326\cdot10^3$
6	$1.8\cdot10^3$	$1.416\cdot10^3$	$1.496\cdot10^3$	$1.188\cdot10^3$	$1.41\cdot10^3$
7	$1.964\cdot10^3$	$1.703\cdot10^3$	$1.762\cdot10^3$	$1.337\cdot10^3$	$1.502\cdot10^3$
8	$2.082\cdot10^3$	$1.891\cdot10^3$	$1.946\cdot10^3$	$1.586\cdot10^3$	$1.681\cdot10^3$
9	$2.144\cdot10^3$	$2.011\cdot10^3$	$2.075\cdot10^3$	$1.854\cdot10^3$	$1.897\cdot10^3$
10	$2.173\cdot10^3$	$2.064\cdot10^3$	$2.161\cdot10^3$	$1.997\cdot10^3$	$2.097\cdot10^3$
11	$2.161\cdot10^3$	$2.081\cdot10^3$	$2.237\cdot10^3$	$2.115\cdot10^3$	$2.223\cdot10^3$
12	$2.193\cdot10^3$	$2.116\cdot10^3$	$2.258\cdot10^3$	$2.207\cdot10^3$	$2.295\cdot10^3$
13	$2.221\cdot10^3$	$2.136\cdot10^3$	$2.243\cdot10^3$	$2.22\cdot10^3$	$2.334\cdot10^3$
14	$2.233\cdot10^3$	$2.176\cdot10^3$	$2.257\cdot10^3$	$2.194\cdot10^3$	$2.333\cdot10^3$
15	$2.268\cdot10^3$	$2.181\cdot10^3$	$2.252\cdot10^3$	$2.162\cdot10^3$	$2.316\cdot10^3$
16	$2.259\cdot10^3$	$2.155\cdot10^3$	$2.255\cdot10^3$	$2.155\cdot10^3$	...

B :=

	1	2	3	4	5
1	924	712	941	719	949
2	950	732	952	746	965
3	970	746	978	752	998
4	995	761	979	766	998
5	$1.015\cdot10^3$	776	991	785	$1.029\cdot10^3$
6	$1.033\cdot10^3$	796	$1.025\cdot10^3$	820	$1.061\cdot10^3$
7	$1.039\cdot10^3$	812	$1.063\cdot10^3$	819	$1.07\cdot10^3$
8	$1.069\cdot10^3$	828	$1.07\cdot10^3$	838	$1.095\cdot10^3$
9	$1.082\cdot10^3$	853	$1.084\cdot10^3$	866	$1.108\cdot10^3$
10	$1.101\cdot10^3$	845	$1.1\cdot10^3$	876	$1.148\cdot10^3$
11	$1.119\cdot10^3$	860	$1.136\cdot10^3$	900	$1.167\cdot10^3$
12	$1.145\cdot10^3$	901	$1.153\cdot10^3$	918	$1.172\cdot10^3$
13	$1.171\cdot10^3$	932	$1.158\cdot10^3$	938	$1.195\cdot10^3$
14	$1.181\cdot10^3$	954	$1.207\cdot10^3$	970	$1.233\cdot10^3$
15	$1.23\cdot10^3$	962	$1.201\cdot10^3$	987	$1.27\cdot10^3$
16	$1.249\cdot10^3$	996	$1.222\cdot10^3$	$1.005\cdot10^3$	...

Figure 7. Image matrices of the level of the IR-camera signal. Size 128x64 pixels

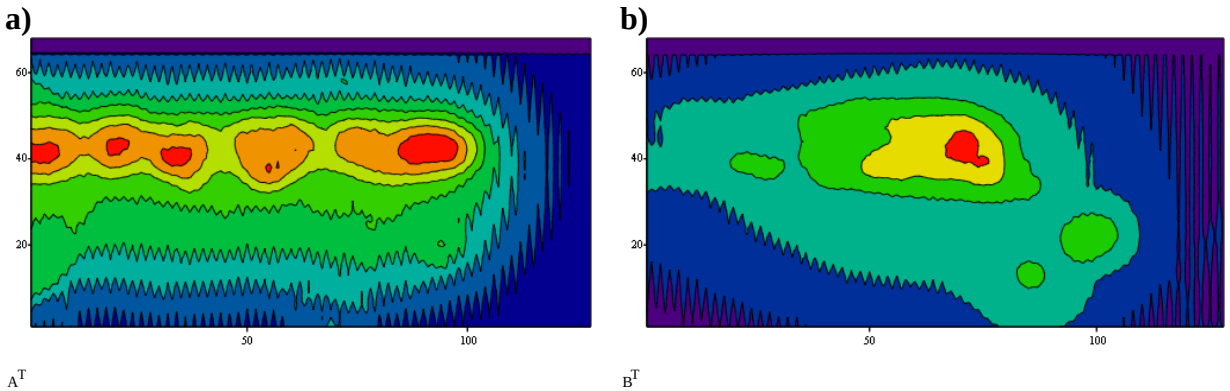

Figure 8. Distribution of the IR-camera signal, corresponding to the process of formation of unstable (a) and stable track (b). Melting parameters: laser power – 30 W, speed (a) – 300 mm / s, (b) – 100 mm / s

According to their morphology, images for 300 and 100 mm/s are very different. It may be noted that it is typical of a higher scanning speed to have several strongly heated regions behind the radiation source, while the speed of 100 mm/s has only one such region. These regions are well described by the melting isotherm, as shown in Figure 6. In this case, the task of controlling the stability of track formation is reduced to recognizing the continuity and uniqueness of the melting isotherm (melting pool).

In the course of the experiments, it was found that the powder particles escaping from the zone of laser radiation either in the direction of scanning or against it, did not fall on the line of the melting pool path. For this reason, a matrix row containing a pixel with the highest value of the digital signal was used for analysis.

So, for matrix A, row 42 was used for processing, and the maximum digital signal value was 4461, for matrix B – a row 43 and a digital signal – of about 5430.

Then, to simplify the image processing procedure and introduce a criterion for recognition of matrices A and B, they were converted to binary ones (Figure 9).

The value of a digital signal corresponding to the melting point of metal powder INOX 316L was set. According to the experiments, a digital signal equal to 3200 conditional units corresponds to the actual temperature value of 1450°C. Using the melting isotherm as the interface between two mediums (liquid/solid), original matrices A and B were reduced to the binary form, based on the condition that the value of matrix elements less than 3200 was replaced by 0, and the value of elements greater than 3200 was replaced by 1. In the program, this was implemented as a cycle.

Figure 9 shows the view of transformed binary matrices f(A) and f(B). Based on the transformation condition, it can be argued that the regions of matrices with zero element values correspond to the solid state of the material, and regions with a value of unity to the liquid state.

After constructing a two-dimensional distribution of elements of matrices f(A) and f(B), clear representation of the geometry of the liquid melt pool was obtained (Figure 10). The image shows that for an unstable melting mode (f(A)) the melting pool looks fragmented and extended, in comparison with the melting pool for a stable mode (f (B)).

f (A) =

	23	24	25	26	27	28	29	30	31	32
34	0	0	0	0	0	0	0	0	0	0
35	0	0	0	0	0	0	0	0	0	0
36	0	0	0	0	0	0	0	0	1	1
37	0	0	0	0	0	0	0	1	1	1
38	1	0	0	0	0	0	1	1	1	1
39	1	1	1	1	1	1	1	1	1	1
40	1	1	1	1	1	1	1	1	1	1
41	1	1	1	1	1	1	1	1	1	1
42	1	1	1	1	1	1	1	1	1	1
43	1	1	1	1	1	1	1	1	1	1
44	1	1	1	1	1	1	1	1	1	1
45	1	1	1	1	1	1	1	1	1	1
46	1	1	1	1	1	1	1	1	1	1
47	1	1	1	1	1	1	1	0	0	0
48	1	1	1	0	0	0	0	0	0	...

f (B) =

	38	39	40	41	42	43	44	45	46	47
32	0	0	0	0	0	0	0	0	0	0
33	0	0	0	0	0	0	0	0	0	0
34	0	0	0	0	0	0	0	0	0	0
35	0	0	1	1	1	1	1	1	1	1
36	0	1	1	1	1	1	1	1	1	1
37	0	1	1	1	1	1	1	1	1	1
38	0	1	1	1	1	1	1	1	1	1
39	0	1	1	1	1	1	1	1	1	1
40	0	1	1	1	1	1	1	1	1	1
41	0	1	1	1	1	1	1	1	1	1
42	0	0	0	1	1	1	1	1	1	1
43	0	0	0	1	1	1	1	1	1	1
44	0	0	0	1	1	1	1	1	1	1
45	0	0	0	1	1	1	1	1	1	1
46	0	0	0	1	1	1	1	1	1	1
47	0	0	0	1	1	1	1	1	1	...

Figure 9. Binary view of image matrices of the level of the IR-camera signal. Size 128x64 pixels

This discreteness of the melt pooling during track cooling leads to the formation of metal spheres.

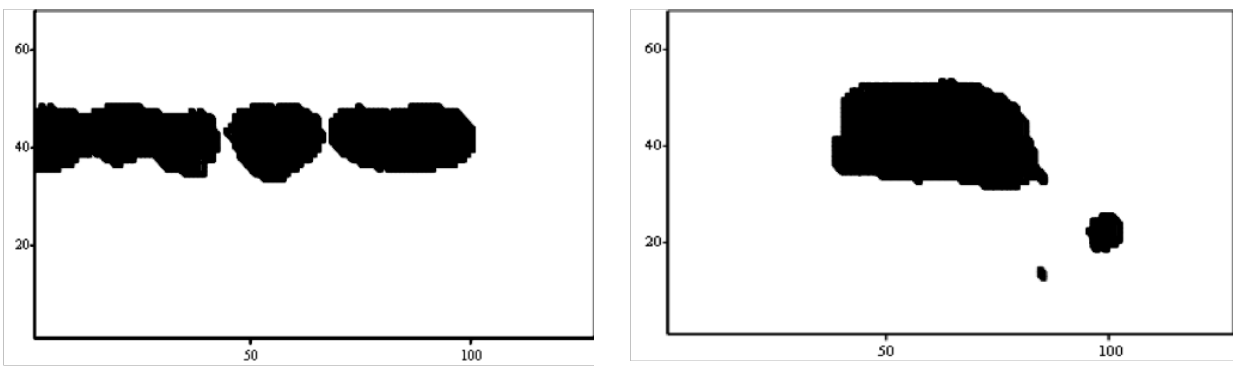

$f(A)^T$ $f(B)^T$

Figure 10. Graphical representation of a binary matrix. The black line corresponds to the melting isotherm of metal powder INOX 316L 1450°C.

The thermal image was analyzed in the row with the maximum digital signal (temperature), therefore, by plotting the distribution of the values in the binary matrix row, the images shown in Fig. 11 were obtained. These graphs show the number of liquid-to-solid phase transitions of the material when analyzing the row with the maximum temperature. Based on the above, the criterion for stable track formation for selective laser melting of INOX 316L metal powder was determined.

This criterion (coefficient K) is the presence of not more than two liquid-to-solid phase transitions in the row with the maximum temperature for thermal image obtained using the IR-camera (Figure 11).

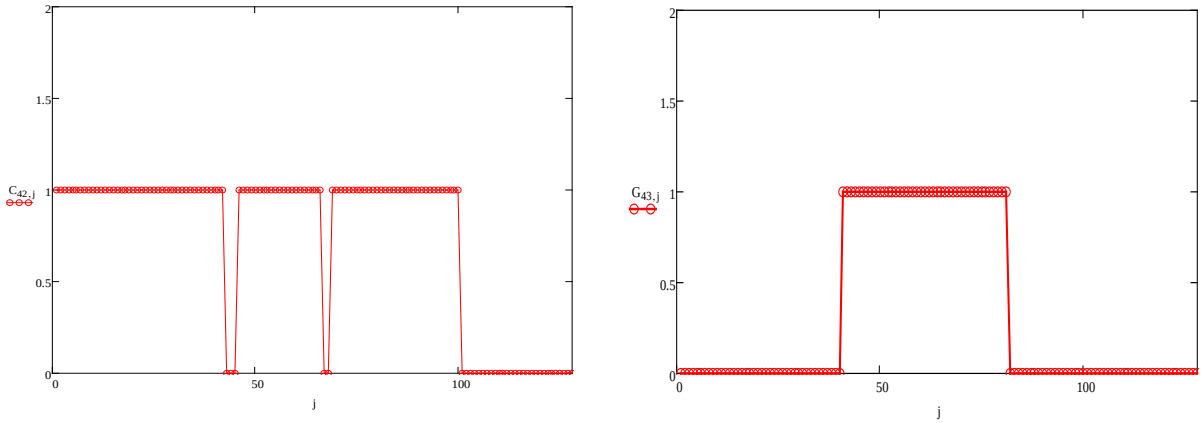

Figure 11. Graphs of the distribution of liquid-to-solid phase transitions of the material in the row with the maximum temperature

If more than two phase transitions are detected in the row with the maximum temperature a signal to change the value of the laser power or scanning speed is sent.

The developed algorithm of the measuring information system was applied in SLM of a multilayer sample (6x6 mm). Stability of the track formation during laser melting was monitored using an IR-camera installed in the working area. At this stage of the control system development, laser power was changed manually. Upon detection the breakage of a melting isotherm on the thermal image (the number of phase transitions in the row with the maximum temperature is greater than 2), the value of laser power was reduced manually.

4 multilayer samples (Figure 12) from CoCr metal powder were formed by successive fusion of single tracks with a step of 50 μm. The average size of powder granules is 20 μm, the thickness of one powder layer is 50 μm. Samples 1 and 3 were produced without control. The following melting parameters were used: scanning speed – 300 mm/s, laser power – 50 W, a number of layers for samples 1, 2 – 10, for samples 3, 4 – 4. For samples 2 and 4, the control system was used. The surface quality improved significantly, the boundaries of the square area became more distinct. A number of irregularities decreased by several times. The roughness curve for samples 3 and 4 is shown in Figure 13. Roughness was measured using the Mod. 252 profilometer. The device is designed to measure surface roughness, the measurement limit is *Ra* = (0,02-250) μm, *Rz* = (0,02-100) μm, accuracy class 1. It can be concluded that for a multilayer sample produced using the control system, the size of the irregularities does not exceed 50 μm. The roughness index *Ra* using the control system for one set of melting parameters was reduced from 39.9 to 6.6 μm.

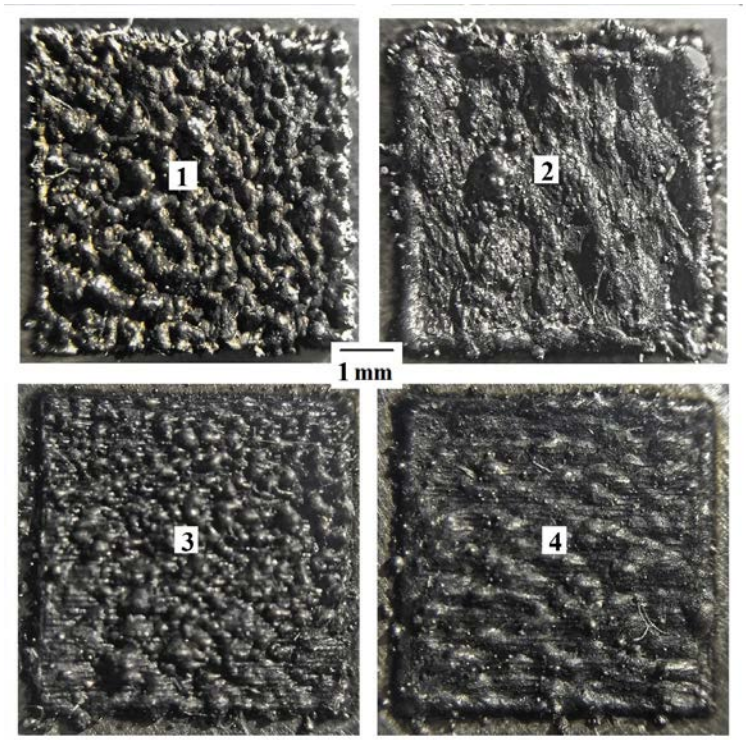

Figure 12. The result of selective laser melting of a multilayer sample (6x6 mm). 1, 3 – by the standard method; 2, 4 – using the developed control system. CoCr metal powder, layer thickness – 50 μm. 1, 2 – 10 layers; 3, 4 – 4 layers. Laser power for 1, 3 – 30 W; for 2, 4 - changed in the process from 50 to 30 W, scanning speed – 300 mm / s

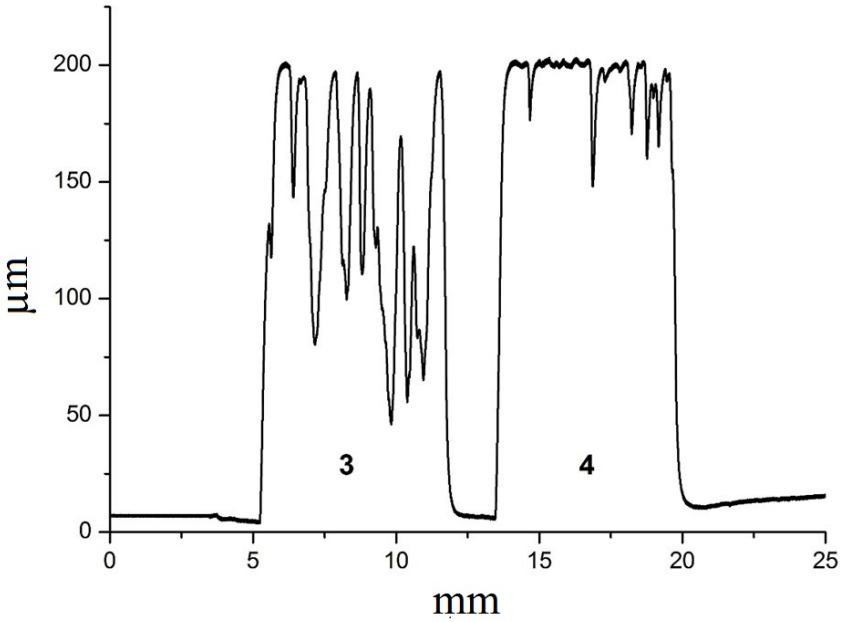

Figure 13. Roughness of the samples obtained by selective laser melting. Sample 3 was produced by the usual method, sample 4 – using the control system

Monitoring system design

Using the developed principle of continuous non-destructive control with morphological analysis of thermal images of the IR-camera, a design and an algorithm for controlling the laser power during SLM were proposed.

To unify and simplify the implementation of the laser power control scheme, it is proposed to use an IR-camera with an Ethernet interface, for example, the Flir SC5200 having the following characteristics:

- InSb detector;
- the resolution of 320x256 pixels;
- frame frequency of up to 11 kHz;
- the spectral range of 2.5-5.1 μm;
- control and data interface - Ethernet (GigE Vision).

Using the developed algorithm of morphological analysis of the thermal image as a function of transforming the processor module, allows creating a design of the measuring information system (Figure 14). The main purpose of this system is to change laser power in the event of deviations during stable track formation.

Coefficient K is responsible for the evaluation of track formation stability in this system. If the numerical value is $K > 2$, an analog signal containing a correction value of laser power is generated. This signal is sent to the controller used in the laser unit.

The correction LP value is selected automatically or set manually by the operator. The choice of the value is based on the preliminary created database of parametric analysis for a specific material. The database contains information about the effect of operating parameters on the single track stability. The initial LP value is set taking into account the known optimal melting modes, including scanning speed, thickness of the powder layer, etc.

The infrared camera installed in the optical system generates an image capturing the zone of laser radiation (melting pool). An image in the form of a two-dimensional matrix, each element of which corresponds to a pixel storing a digital signal value, enters the processor module. Then, according to the algorithm described earlier, coefficient K is calculated.

To process the image and generate a correcting signal, a control processor is used based on the CPC308-01 processor module with two Ethernet interfaces.

The special feature of the CPC308-01 processor module is the presence of two Ehternet controllers on board, which makes it easy to integrate it into the laser power control scheme.

Based on the results obtained, together with Dr. A. Laskin (AdlOptica Optical Systems GmbH), an optical circuit for integration of an IR-camera into the optical path of the SLM machine was developed. (Figure 15).

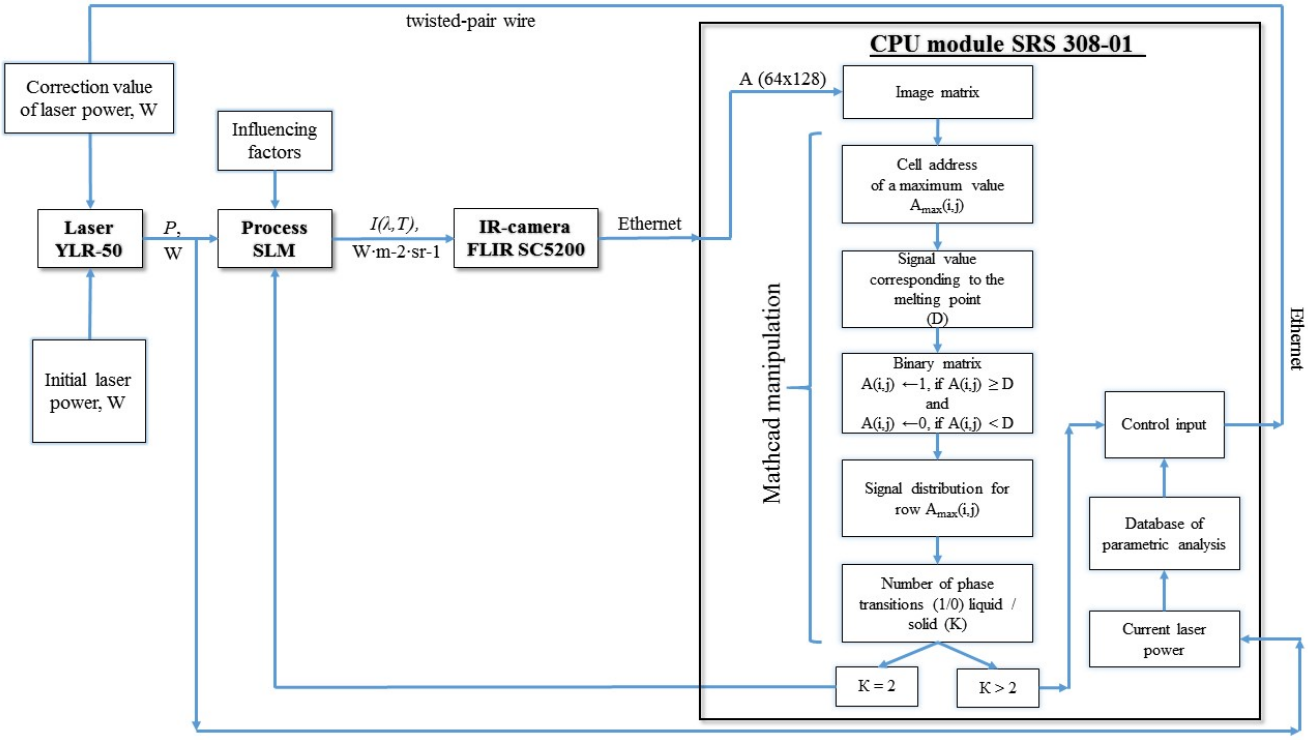

Figure 14. Design of the measuring information system for SLM control based on morphological analysis of the thermal image.

The difference of this optical system lies in the absence of a focusing F-theta lens, usually located behind the 2D scanning device. Its role is performed by focusing optics with movable lenses, varioSCAN developed by Scanlab. Such circuit is implemented because optics of the system should pass not only the laser wavelength, but also the IR-camera wavelengths. Making lenses for small varioSCAN is much less expensive than for a focusing F-theta lens.

This configuration allows real-time monitoring of the zone of laser radiation. This is ensured by the fact that the laser beam and the field of view of the IR camera focus coaxially in one focal plane using a single optical system.

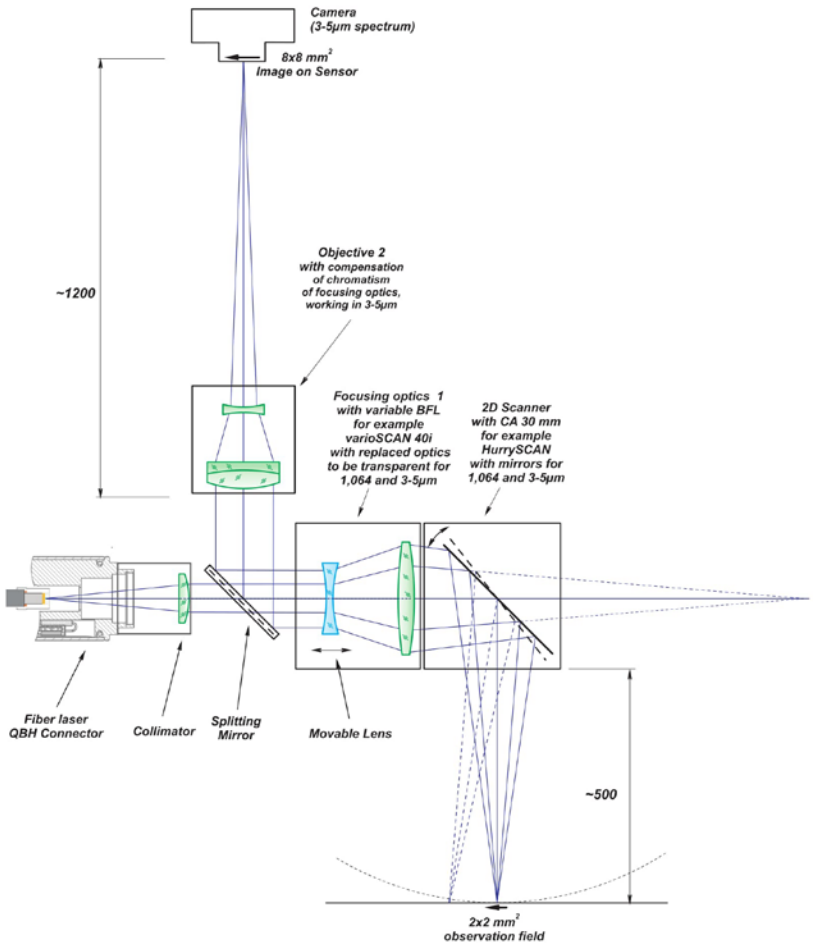

Figure 15. Design of integrating the IR-camera into the optical system of the selective laser melting machine

Conclusion

Morphological analysis of the thermal image revealed the sign of formation of an unstable track (its degradation). Disturbance of process stability occurs when the melting isotherm is “fragmented”, i.e. increase in the number of liquid/solid interfaces along the line with the maximum temperature.

Recommendations are given for integration of a measuring information system using an IR-camera in the optical path of a SLM machine. The principle of continuous non-destructive control with feedback for controlling laser power based on morphological analysis of thermal images is proposed.

The obtained results and recommendations can be applied in development and manufacture of industrial SLM machines with an integrated active control system.

References

1. M. Doubenskaia, M. Pavlov, Y.Chivel. Optical system for on-line monitoring and temperature control in selective laser melting technology // Key Engineering Materials. – 2010. – V. 437. – P. 458-461.
2. T. Craeghs, F. Bechmann, S. Berumen, J.-P.Kruth. Feedback control of Layerwise Laser Melting using optical sensors // Proceedings of LANE 2010: 6th International Conference on Laser Assisted Net Shape Engineering. – V. 2 –, 2010. – P. 506-514.
3. I.Smurov. Laser process optical sensing and control // IV International WLT-Conference on Lasers in Manufacturing – Munich, 2007. – P. 537-546.
4. I. Smurov, M.Doubenskaia. Temperature monitoring by optical methods in laser processing // Laser-Assisted Fabrication of MaterialsSpringer-Verlag Berlin Heidelberg, 2013. – P. 373-422.
5. I. Yadroitsev, P.Bertrand, I.Smurov. Parametric analysis of selective laser melting technology // Applied Surface Science –2007. – V. 253, № 19. – P. 8064-8069.
6. I. Yadroitsev, I. Yadroitsava, I.Smurov. Strategy of fabrication of complex shape parts based on the stability of single laser melted track // SPIE LASE. – International Society for Optics and Photonics. – 2011. – P. 79210P-13.
7. T. Vilaro, S. Abed, W.Knapp. Direct manufacturing of technical parts using selective laser melting: example of automotive application // Proc. of 12th European Forum on Rapid Prototyping –, 2008.
8. E. Yasa, J. Deckers, J.P.Kruth. The investigation of the influence of laser re-melting on density, surface quality and microstructure of selective laser melting parts // Rapid Prototyping Journal. – 2011. – V. 17, T. 5. – P. 312-327.
9. I. Zhirnov, I. Yadroitsava, I.Yadroitsev. Optical Monitoring and Numerical Simulation of Temperature Distribution at Selective Laser Melting of Ti6Al4V Alloy // Materials Science Forum. – V. 828 –Trans Tech Publications, 2015. – P. 474-481.
10. M. J. Matthews, G. Guss, S. A. Khairallah, A. M. Rubenchik, P. J. Depond, King W. E. Denudation of metal powder layers in laser powder bed fusion processes // Acta Materialia. – 2016. – V. 114. – P. 33-42.
11. R. Li, J. Liu, Y. Shi, L. Wang, W.Jiang. Balling behavior of stainless steel and nickel powder during selective laser melting process // The International Journal of Advanced Manufacturing Technology. – 2012. – V. 59, № 9-12. – P. 1025-1035.
12. D. Gu, Y.Shen. Balling phenomena in direct laser sintering of stainless steel powder: metallurgical mechanisms and control methods // Materials & Design. – 2009. – V. 30, № 8. – P. 2903-2910.
13. J.-P. Kruth, L. Froyen, J. Van Vaerenbergh, P. Mercelis, M. Rombouts, B.Lauwers. Selective laser melting of iron-based powder // Journal of Materials Processing Technology. – 2004. – V. 149, № 1. – P. 616-622.